Journal of Harbin Engineering University
ISSN: 1006-7043

Vol 46 No. 12
December 2025

Application of Kolmogorov-Arnold Networks in Drought Prediction: A Comparison with Artificial Neural Networks using SPEI

Angel R [1], Kokila Ramesh [2], Anita Chaturvedi [3], Kumudha H R [4]

[1] Research Scholar, JAIN - (Deemed to be University), Bangalore, Karnataka, India

[2] Associate Professor, Faculty of Engineering and Technology, Jain (Deemed-to-be University), Bangalore, Karnataka, India

[3] Professor, Faculty of Engineering and Technology, Jain (Deemed-to-be University), Bangalore, Karnataka, India

[4] Assistant Professor, Bharathi College PG & RC & Founder of StatMint Innovations

[MSME URNO: UDYAM-KR-21-0055049] Mandya, Karnataka, India. Email: kumudhamayur@gmail.com & statmintinnovations@gmail.com

Abstract

The incidence of droughts has increased markedly in the recent years and their adverse impact has significantly disrupted the ecosystem. Therefore, there is a compelling need to address these alarming challenges. Drought prediction tools can aid in mitigating the effects of droughts. Artificial intelligence methods and data driven models have enhanced the predictive capabilities of the complex drought models. This study presents the application of Kolmogorov Arnold Network (KAN) model to predict the drought events using the Standardised Precipitation Evapotranspiration Index (SPEI). This model is compared to the Artificial Neural Network (ANN) model using the NASA POWER data for the drought prone regions of Bankura, Bagalkot, Mewat and Jaisalmer. The target variable SPEI is derived using the Pen Montieth equation for potential evapotranspiration and precipitation. A custom weighted Huber Loss function is used to emphasize the drought episodes in the prediction. Results demonstrates that both the models successfully capture the nonlinear relationships between the SPEI and the input variables. The developed models show a similar predictive capability with high RMSE (0.09-0.21) and R^2 (more than 0.94) values. The difference in the performances of the model is very negligible. This study highlights that KAN can be robust alternative to ANN for regional drought forecasting. The findings of the paper will help the agricultural community and the government agencies to monitor droughts and aid in mitigating its induced effects.

Keywords: Kolmogorov -Arnold Network, ANN, Modelling, ANN, Droughts, SPEI.

Highlights:

- Kolmogorov – Arnold Network (KAN) is applied for the prediction of regional droughts.
- KAN and ANN are compared for drought forecasting using Standardised Precipitation Evapotranspiration Index (SPEI).
- Bothe models effectively capture the non- linear relationship between the input data and SPEI
- The study finds that KAN is a robust alternative to ANN for drought prediction.

1. Introduction

Drought is one of the most hazardous events of nature. The impact of droughts, causes an imbalance in the demand and the supply of water, affecting the water needs of the ecosystem. The occurrence of droughts in the recent years is attributed to reduced rainfall and the abnormalities in the temperature [1]. There is an increase of 0.2^0C in the global temperature per decade in the past 30 years [2]. The climate variability and the anthropogenic activities have induced the occurrence of droughts. In the semi-arid regions of Iran, the climate change has significantly affected the severity, duration and frequency of the droughts [3]. The increase in the frequency of drought due to climate change has affected the plant growth in Central Poland [4]. Furthermore, an ensemble of 9 CMIP6 models, show that in the large parts of Africa, Asia and America, the anthropogenic activities also act as the drivers of the drought [5]. Accurate prediction of droughts is essential for water resource

management and agricultural activities. Therefore, drought forecasting becomes an indispensable tool to monitor and mitigate droughts

Droughts are defined as the prolonged period of dryness due to lack of rainfall in its natural climate. According to Wilhite and Glantz, there cannot be a universal definition of drought [6]. The lack of single definition of drought, makes it difficult to determine its onset and termination. Droughts can be classified based on its intensity as meteorological, agricultural, hydrological and socio-economic droughts [7].

Drought prediction involves using appropriate input data, a suitable drought index and an accurate model [8]. The input data can be broadly classified as station-based data, satellite-based data and remote sensing data. With the increasing climate change, the use of datasets from Climate Research Unit (CRU) and CHIRPS has enhanced the regional drought prediction [9,10,11]. Using one of the drought indicators such as temperature, precipitation, soil moisture etc. or a combination of it, the drought index is obtained. Some of the common drought indices are the Standardised Precipitation Index (SPI), Standardised Precipitation Evapotranspiration Index (SPEI), China Z-Index, Aridity Index, Palmer Drought Severity Index (PDSI), etc [12,13,14,15]. SPI is the index which is recommended by the World Meteorological Organisation due to its simplicity in its computation. It requires only precipitation as the input variable. Though the precipitation is relative same over the years, due to the rise in the temperature, the frequency of droughts has increased leading to the decrease in the agricultural productivity [16]. The SPEI index combines precipitation and temperature and is sensitive to global warming, is also widely used to evaluate droughts [17]. SPEI was able to estimate the soil moisture with higher accuracy, when compared to SPI with the accuracy of 36% [18].

The drought models can be physical models or data driven models. The physical models are based on the physical process like the atmospheric water cycle, soil type and runoffs. Data driven models learn patterns or relationship between the variables using the historical data. With the advancement of artificial intelligence, the complex non-linear patterns in the variables of the droughts can be identified using statistical or machine learning techniques. Some of the data driven models used are the regression models, Artificial Neural Network models, Support Vector Machines (SVM), Random Forest, Long Short-Term Memory model, etc [19,20,21,22,23]. The deep learning models such as the ANN is widely used for the prediction of droughts and other extreme events. ANN has been effectively used to predict the floods in India [24]. Other models such as Gaussian mixture model and a non-Gaussian model are applied to predict floods and drought in the coastal regions of Karnataka using ANN models achieving good accuracy [25,26,27]. To understand the intensity, variability and the seasonal patterns the probability distributions of the rainfall of the region of Karnataka is studied [28, 29, 30,31]. Although many models such as ANN, SVM, Random Forest are widely used, Kolmogorov-Arnold Network (KAN) based on the Kolmogorov-Arnold representation theorem is rarely used to explore droughts [32,33,34]. Therefore, the primary objective of this study aims to study and compare the KAN and ANN models to forecast droughts using SPEI across four drought prone regions in India.

2. Materials and Methods

2.1. Study Area

Jaisalmer is a city located in Rajasthan, in the western part of India. It is an arid region, bordered by Jodhpur, Bikaner, Barmer, and Pakistan, and is part of the Thar Desert. The region lacks perennial rivers, and the Indira Gandhi Canal is utilized for irrigation [35]. Mewat district is situated in Haryana, in northern India. It is bordered by the districts of Gurgaon, Rewari, and Faridabad, as well as Rajasthan. The topography is characterized by upland lowland, and agriculture is primarily rain-fed, resulting in a comparatively low production per hectare with variable climate [36]. Bankura, a district in West Bengal situated in the western region of India and is prone to frequent droughts [37]. It holds the highest rank among the districts in West Bengal in terms of drought susceptibility. The area is characterized by high evaporation rates and low precipitation, resulting in reduced moisture levels. The Bagalkot district of Karnataka is one of the drought-prone regions of the state, situated in the southern part of the country [38]. Table 1 presents the geographical co-ordinates and the climate of the regions.

Table 1: Study regions and their geographical locations. The table lists the selected study regions along with their corresponding states, geographical coordinates (latitude and longitude in degrees), and dominant climatic conditions.

Region	State	Latitude(^{0}N), Longitude (^{0}E)	Climate
Jaisalmer	Rajasthan	26.92 and 70.93	arid
Mewat	Haryana	27 and 76.9	Semi- arid
Bankura	West Bengal	23 and 87	Wet & dry
Bagalkot	Karnataka	16.18$^{0°}$and 75.7	Semi-arid

2.2. Methodology

Figure 1. The general framework of the research is presented. It presents the overall workflow of the study, including data acquisition, preprocessing, SPEI computation, model training, and performance evaluation.

2.2.1. Data

The datasets employed in this research originated from $0.5^0 \times 0.5^0$ datasets at a specific location, determined by the latitude and longitude coordinates accessible via the National Aeronautics and Space Administration (NASA) "POWER Single Point Data Access Widget," which offers access to data [39]. The agency uses ground-based sensors, computational models, and a network of satellites to gather data. This approach enables NASA to provide information regarding climate change and trends. The datasets for the years 1984–2023, encompassing 40 years is used in this analysis.

2.2.2. Standardised Precipitation Evapotranspiration Index (SPEI)

The Standardised Precipitation Evapotranspiration Index considers precipitation and evapotranspiration as the drought indicators. The inclusion of temperature in quantifying drought makes it more responsive to the climate change, while SPI uses only precipitation and is not considering the dry effects, due to rise in the temperature [40]. SPEI is calculated by considering the water balance which is the difference between the precipitation and potential evapotranspiration. Potential evapotranspiration is obtained using Pen-Montieth equation given by equation (1)

$$ET_0 = \frac{0.408\Delta(R_n - G) + \gamma \frac{900}{(T+273)} U_2(e_s - e_a)}{\Delta + \gamma(1 + 0.34\, U_2)} \quad (1)$$

Where ET_0: reference evapotranspiration (mm/day), Δ: slope of saturation vapor pressure curve (kPa/°C) Rn: net radiation at the crop surface (MJ/m²/day), G: soil heat flux density (MJ/m²/day) — often ≈ 0 for daily time steps, T: mean daily air temperature at 2 m height (°C), U_2: wind speed at 2 m height (m/s), e_s: saturation vapor pressure (kPa), e_a = actual vapor pressure (kPa), γ: psychrometric constant (0.0677) ((kPa/°C)

The water balance, which is the difference between the precipitation and evapotranspiration obtained is fitted in a log logistic distribution and the cumulative distribution function is obtained. Then the values are normalised to obtain the final SPEI values. The SPEI values are classified to be extreme droughts, if SPEI < -2, Severe drought, if -2<SPEI<-1.5, mild drought, if -1<SPEI<-0.5 and no droughts if -0.5 < SPEI<0.5 and wet for the remaining values [41, 42].

2.3. Data Preprocessing and Exploratory Analysis

The dataset obtained from NASA is analysed for missing values and the infinite values. The target variable SPEI, is derived for the monthly timescale [43]. The required time series including the input variable and the target variable is prepared for this study.

To understand the strength of the linear relationship between the input variables and the target variable SPEI, the correlation matrix is obtained. Figure 1, represents the correlation matrix of Bankura district. The correlation coefficient of SPEI with precipitation, specific humidity and temperature are 0.81, 0.87 and

0.085 respectively. Similarly, for the Mewat region the correlation co-efficient for precipitation, specific humidity and temperature are found to be 0.67, 0.52 and -0.35 respectively. In the Bagalkot district of Karnataka, the correlation coefficients are 0.82, 0.77, and -0.55 for precipitation, specific humidity, and temperature with SPEI-1, respectively. For the Jaisalmer region, the correlation values are 0.27, -0.33, and -0.77 for temperature, specific humidity, and temperature respectively [44]. Further, the data is normalised using the Standard scalar scaling technique for data analysis. The data was split chronologically to maintain the temporal dependencies [45].

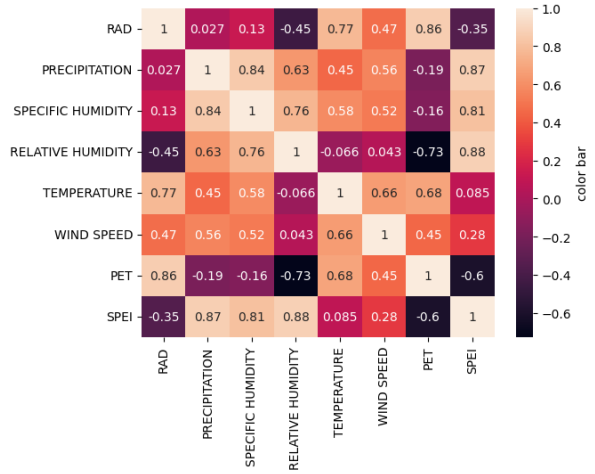

Figure 2. Correlation matrix for Bankura district of West Bengal of the climate variables and SPEI. The heat map summarises the interaction pattern among the temperature, relative humidity, windspeed temperature, precipitation, radiation and SPEI

2.4. Modelling

2.4.1. Artificial Neural Network Model (ANN)

ANN is a computational model based on the structure and the function of the human brain. Just as the information is passed through the neuron in the brain, ANNs are interconnected layers of neuron to process the data and learns the complex non-linear patterns and the relationship between the variables [46]. It consists of three layers- the input layer, hidden layer and the output layer. The input layer receives the pre-processed and the normalised data. The hidden layer performs non-linear transformations using weights and the activation functions. The output layer predicts the model values [47]. Determining the optimal number of neurons and the number of hidden layers is the challenge in designing a neural network. The weights and biases are optimised using back propagation algorithms. The various activation functions used are the ReLu, sigmoid function, swish function and so on [48]. The Adam optimiser is employed to optimise the parameters. There is no standard method to select an appropriate architecture. If the network is too small then the model suffers from underfitting. And if it is a complex architecture, then it suffers from overfitting [49].

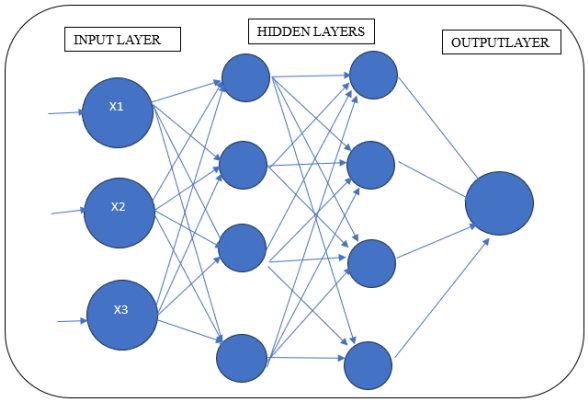

Figure 3. Architecture of a feedforward artificial neural network (ANN). The network consists of an input layer two hidden layers with nonlinear activation function, and an output layer producing the predicted output.

2.4.2. Kolmogorov – Arnold Network (KAN)

Kolmogorov – Arnold Network (KAN) is a recently developed neural network, based on Kolmogorov – Arnold Theorem. It states that any continuous multivariate function can be expressed as the finite sum of the univariate functions applied to linear combinations of the input co-ordinates [50,51,52]. Mathematically, a continuous function $f: [0,1]^n \rightarrow \mathrm{R}$, can be expressed in KAN as (2)

$$f(x_1, x_2, x_3, \dots, x_n) = \sum_{q=1}^{2n+1} g_q \left(\sum_{p=1}^{n} \varphi_{p,q}(x_p) \right) \qquad (2)$$

Where $x_i \in [0,1]$ are the inputs, g_q represents the outer transformation applied to each block and each $\varphi_{p,q}(x_p)$, represents inner univariate transformation. Each input passes through the univariate non-linear map given by (3)

$$\varphi_{p,q}(x_p) = a_{pq} \tanh(x_p) + b_{pq} \qquad (3)$$

Where $a_{pq}\ and\ b_{pq}$ are the weights and biases applied to input variable. For each q, the transformed co-ordinates are summed given by (4)

$$s_q(x) = \sum_{p=1}^{n} \varphi_{p,q}(x_p) = \varphi_{1,q}(x_1) + \varphi_{2,q}(x_2) + \varphi_{3,q}(x_3) + \cdots \qquad (4)$$

Each of the sum, is passed through the non-linear outer transformation as

$$g_q\left(s_q(x)\right) = c_q \tanh\left(s_q(x)\right) + d_q \qquad (5)$$

Where c_q *and* d_q are learnable weights and biases. The final output is the sum of outer functions $g_q(.)$,

$$f(x) = \sum_{q=1}^{2n+1} g_q\left(s_q(x)\right) \qquad (6)$$

This is the Kolmogorov additive decomposition of the model

$$f(x_1, x_2, x_3, \ldots, x_n) = \sum_{q=1}^{2n+1} g_q\left(\sum_{p=1}^{n} \varphi_{p,q}(x_p)\right) \qquad (7)$$

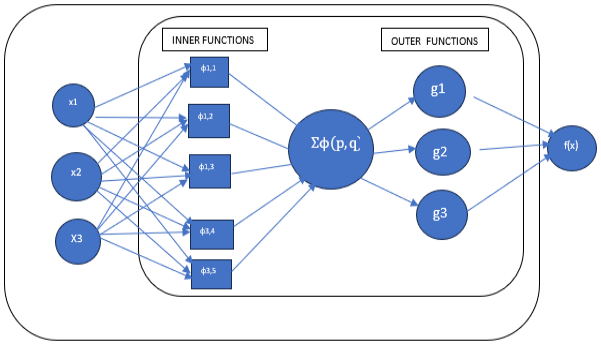

Figure 4. Schematic representation of the Kolmogorov–Arnold Network (KAN) architecture showing the inner univariate spline functions $\boldsymbol{\phi_{p,q}(x_p)}$, summation layer, and outer function $\boldsymbol{g_q}$

Each input feature x_p, is processed through inner transformation $\varphi_{p,q}(.)$ generating the non-linear response. That is, the function applies non-linear 'tanh' transform to the input x_p, to form one inner univariate component of the KAN decomposition as given by equation (3). Then for each block 'q', the co-ordinates are added and a sum is obtained, represented by equation (4). This is the structure of KAN theorem. Each sum is then passed on through the univariate non-linear function given by $g_q(.)$ given by equation (5). They capture the interactions among different dimensions from the previous step. The overall output is obtained by summing all the outer transformations as represented by equation (6). They capture the non-linear mapping by combining the transformed representations generated by the inner and the out layers.

2.4.3. Model Training

The model is trained on 80 % of the data and remaining 20% is used for testing. A chronological split is considered for temporal dependencies. The input variables and the target variable SPEI are standardised using the Standard Scaler. Both the models ANN and KAN use the Adam optimiser with the learning rate of 0.001 for a better optimisation. A custom weighted Huber loss function is used to emphasise the negative values of SPEI. Weights of 3.0 is applied to negative SPEI values to penalise the underestimation [53].

Both the models are trained for 200 epochs and with a batch size of 32, and validation was done using the test dataset with three input feature – temperature, precipitation and specific humidity. The KAN model considered had 5 inner univariate function and 3 outer functions with tanh as the activation function. The ANN model consists of two hidden layers with 64 and 32 neurons respectively, with 'tanh' as the activation functions. For the KAN model, the activation function is replaced by learnable univariate functions which act as the neural approximations. Back propagation is used to update weights and reduce the custom weighted Huber loss. The model was implemented using Python with NumPy, Scikit and Keras on Google Colab platform

2.4.5. Model Evaluation

The performance of the KAN and ANN models are evaluated using the metrices: Root Mean Square (RMSE) and the co-efficient of determination (R^2) [54]

$$R^2 = 1 - \frac{\sum_{i=1}^{n}(y_i - \widehat{y_i})^2}{\sum_{i=1}^{n}(y_i - \overline{y_i})^2}$$

$$RMSE = \sqrt{\frac{1}{n}\sum_{i=1}^{n}(y_i - \hat{y}_i)^2} \qquad (8)$$

where 'n' is the total number of observations, y_i is the actual value, $\hat{y}_i$ is the predicted value and $\overline{y_i}$ is the mean of all the actual values. The models with lower RMSE and MAE, and higher R^2 is considered to be a better predictive model.

The loss curve is another tool to evaluate the learning behaviour and the generalising capacity of the model during the training period. It is a visual tool to gauge how well model performs during the training and the validation.

Scatter plots between observed and predicted values during the testing period is used to visualize model performance

3. Results and Discussion

This paper involves the study of the predictive capabilities of KAN model and ANN model with respect to the Standardised Precipitation Evapotranspiration Index (SPEI). The models are trained with 80% of time series with the same input variables- Precipitation, temperature and specific humidity for both the models. The model was evaluated using the metrics; Root Mean Square Error (RMSE), Co-efficient of determination (R^2) and Mean Absolute Error.

In KAN, each input feature is passed on to learnable dense network, with 'tanh' functions, that are approximations of the univariate mapping. Then these outputs of these are summed across all input features. Each of these sums are passed on the second dense block of 'tanh' functions performing the outer transformations. The outer units produce the nonlinear interactions among the summation of the univariate transformation. The final output is obtained by combining all the responses of the outer functions. KAN helps to detect the influence of a single variable and the group of variables that influence the output. In this paper, 'tanh' is used for the transformations, while other transformations such a wavelet is used instead of the traditional spline function. [55].

The ANN model consisting of input layer, two hidden layers with 64 and 32 neurons and the output layer. The activation function 'tanh' is considered to capture the non-linear patterns. Custom weighted Huber loss and the higher penalties for negative SPEI is applied. ANN provides a non-linear approximation for the relationship between the input variables and the target variables focusing on drought episodes.

The performance of the model during the training period is presented in the Table 2. Both models have captured the relationship existing between the input variable – temperature, precipitation and specific humidity and SPEI. The RMSE during the training period for the four regions are between 0.09 and 0.20 and the R^2 values range between 0.99 to 0.95, explaining more than 95% of the variance for both the models. The correlation co-efficient is as high as 99% in both the cases during the training period. Bankura and Mewat has lowest of the RMSE capturing the drought pattern effectively, while Jaisalmer has the highest RMSE due to the variability in the climate, the model performance is robust. The predictive accuracy is more than 95%, indicating that both the models are performing equivalently well across all regions in replicating SPEI, with minor deviations during extreme dry or wet events.

Table 2: Training performance metrics of KAN and ANN models across four regions

	KAN			ANN		
Regions	RMSE	R^2	Correlation	RMSE	R^2	Correlation
Bankura	0.0990	0.9901	0.99	0.0923	0.9914	0.99
Jaisalmer	0.2039	0.9561	0.98	0.1970	0.9590	0.98
Mewat	0.1402	0.9806	0.99	0.1270	0.9840	0.99
Bagalkot	0.1308	0.9816	0.99	0.1340	0.9807	0.99

This table compares the training performance of the KAN and ANN models for drought prediction in Bankura, Jaisalmer, Mewat, and Bagalkot. The performance indicators include RMSE, R^2, and correlation coefficient (r), indicating how well each model fits the training data.

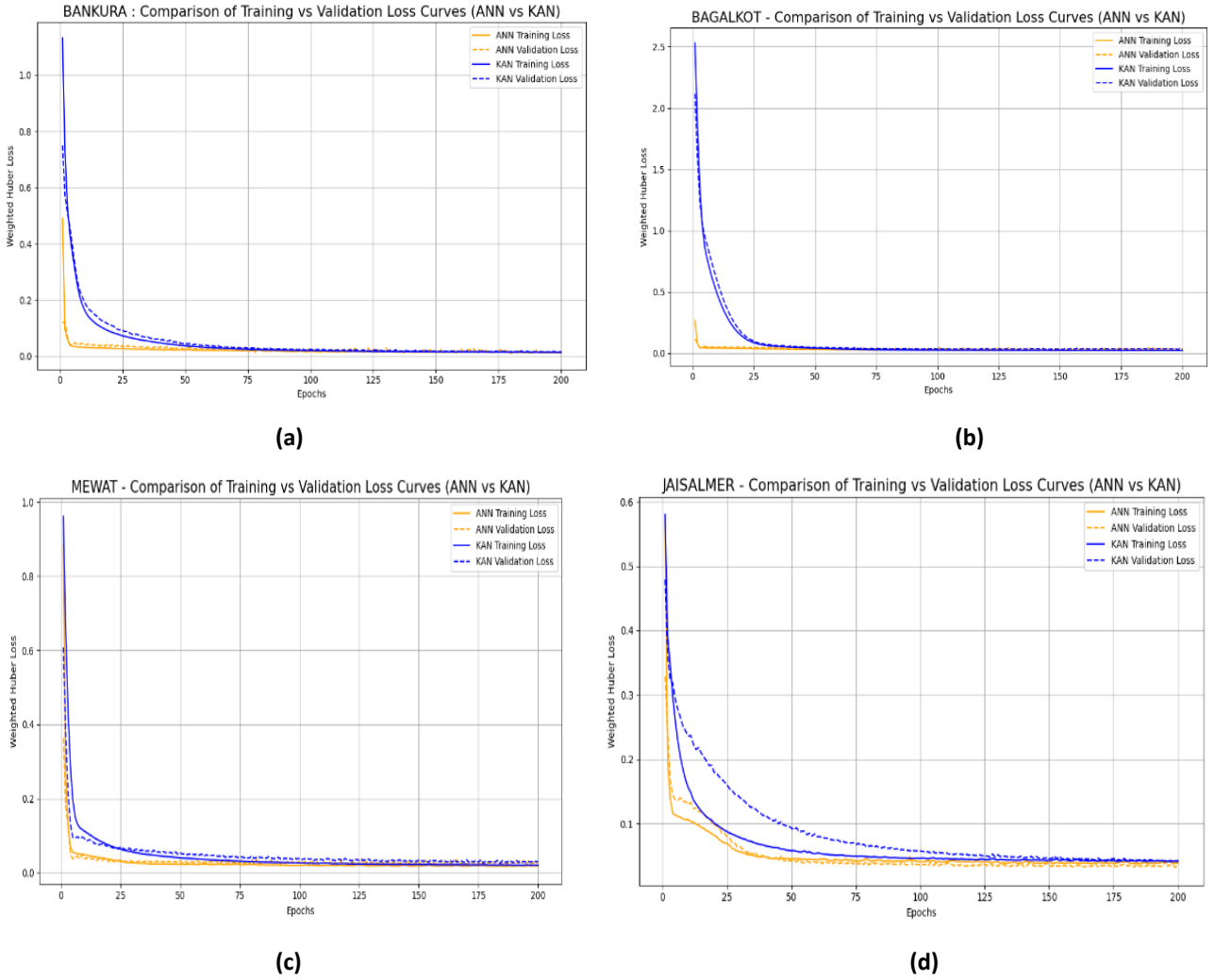

Figure 4. Training and validation loss curves for ANN and KAN models across the four study regions. Comparison of Weighted Huber Loss for Artificial Neural Network (ANN) and Kolmogorov–Arnold Network (KAN) models over 200 epochs for (a) Bankura, (b) Bagalkot, (c) Mewat, and (d) Jaisalmer

The training and the validation loss represented by Figure 4, indicate the both the models converge smoothly, with stable learning and minimum overfitting, indicating good generalisation to the unseen data. The loss decreases quickly and stabilises at the lower values, concluding that the both models are not suffering from high bias or variance.

The performance of the KAN and ANN models during the test period is presented in the table 2. The RMSE is the lowest for the Bankura region and is highest at Jaisalmer for both the models. With all the R^2 values is more than 94% of the variance is explained by the model. The correlation co-efficient is more than 98% for the models. The difference in the RMSE values for both the models is minimal, indicating that ANN is sufficient for the drought prediction, when compared to KAN model

Table 2: Testing Performance Metrics of KAN and ANN Models Across Four Regions

Regions	KAN			ANN		
	RMSE	R^2	Correlation	RMSE	R^2	Correlation
Bankura	0.0952	0.9882	0.99	0.1009	0.9867	0.99
Jaisalmer	0.2158	0.9466	0.98	0.1922	0.9576	0.98
Mewat	0.1717	0.9661	0.99	0.1486	0.9746	0.99

Bagalkot	0.1739	0.9700	0.99	0.1572	0.9755	0.99

This table presents the testing results for KAN and ANN models across the same four regions. It highlights the predictive capability and generalization performance on unseen data, showing that both models perform consistently with minor regional deviations.

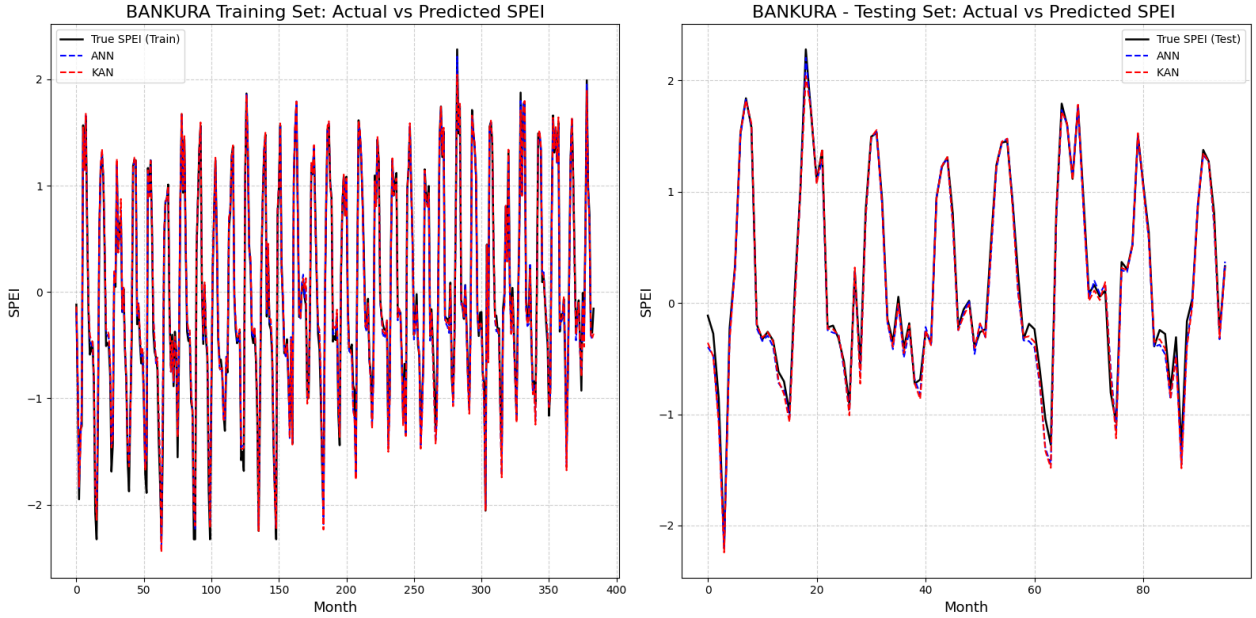

Figure 5. Comparison between observed and predicted SPEI values using ANN and KAN models for the Bankura region

Both models show a close agreement with observed data during the testing period, indicating strong predictive capability in capturing regional drought variability.

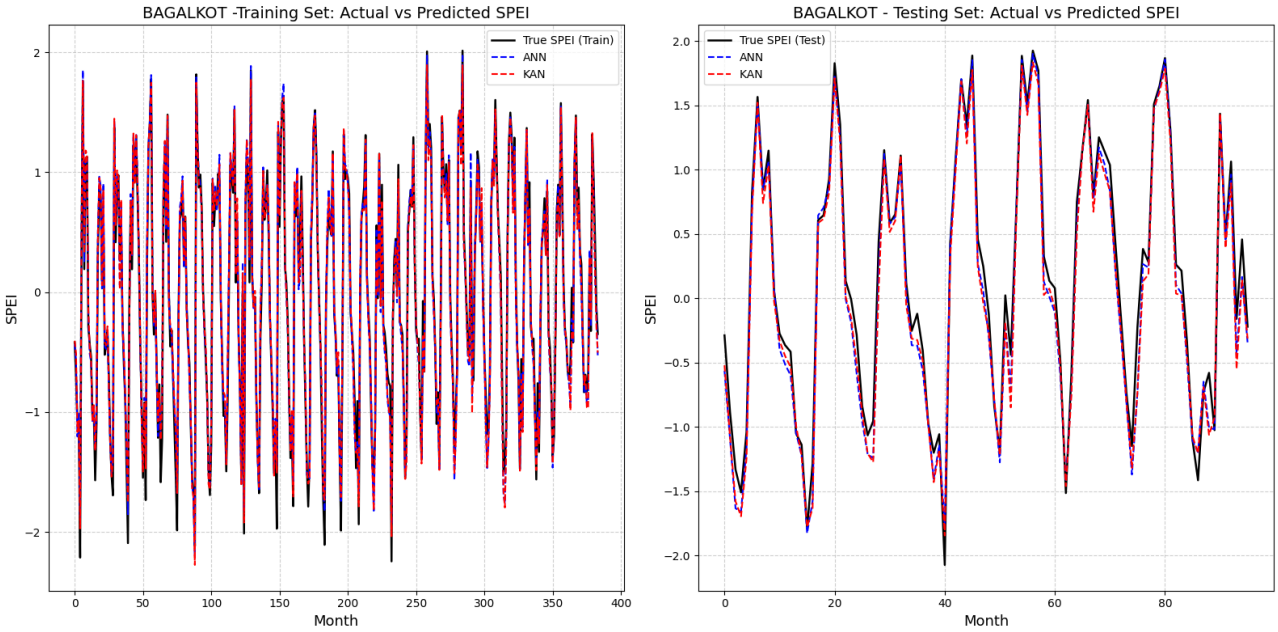

Figure 6. Observed and predicted SPEI trends for the Bagalkot region

Both ANN and KAN models show high predictive capability and temporal consistency, successfully replicating observed drought dynamics in the testing period

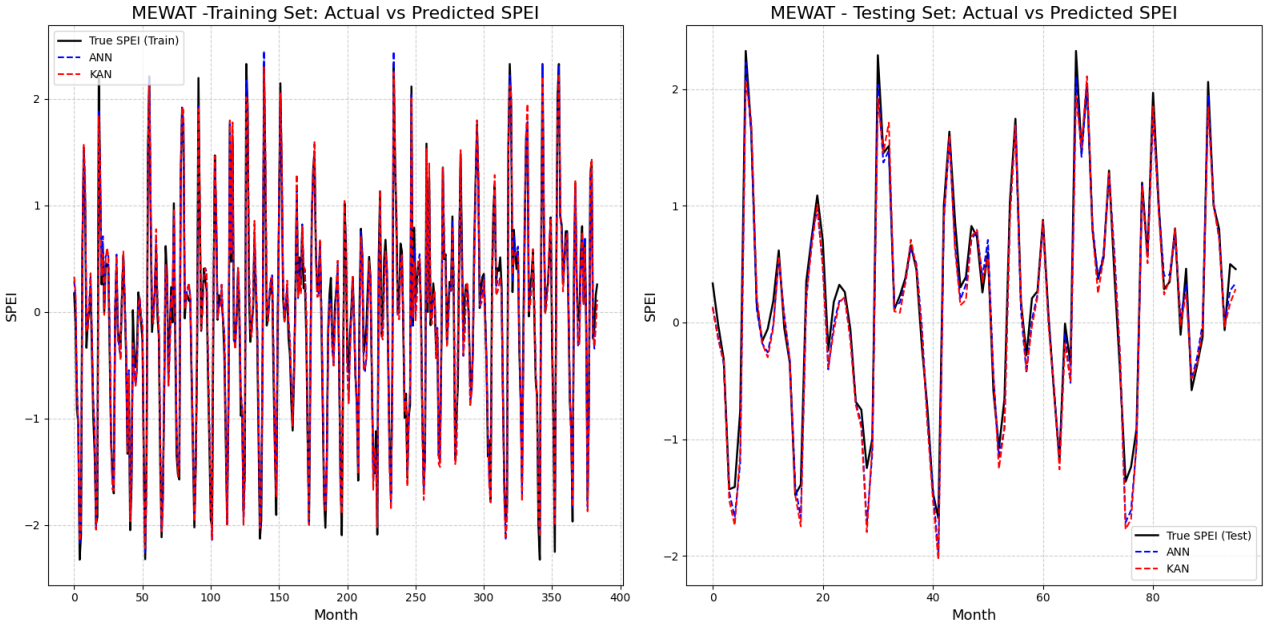

Figure 7. Time-series comparison of observed and predicted SPEI for the Mewat region

The KAN model exhibits smoother temporal transitions compared to the ANN, indicating enhanced ability to model drought persistence and recovery phases.

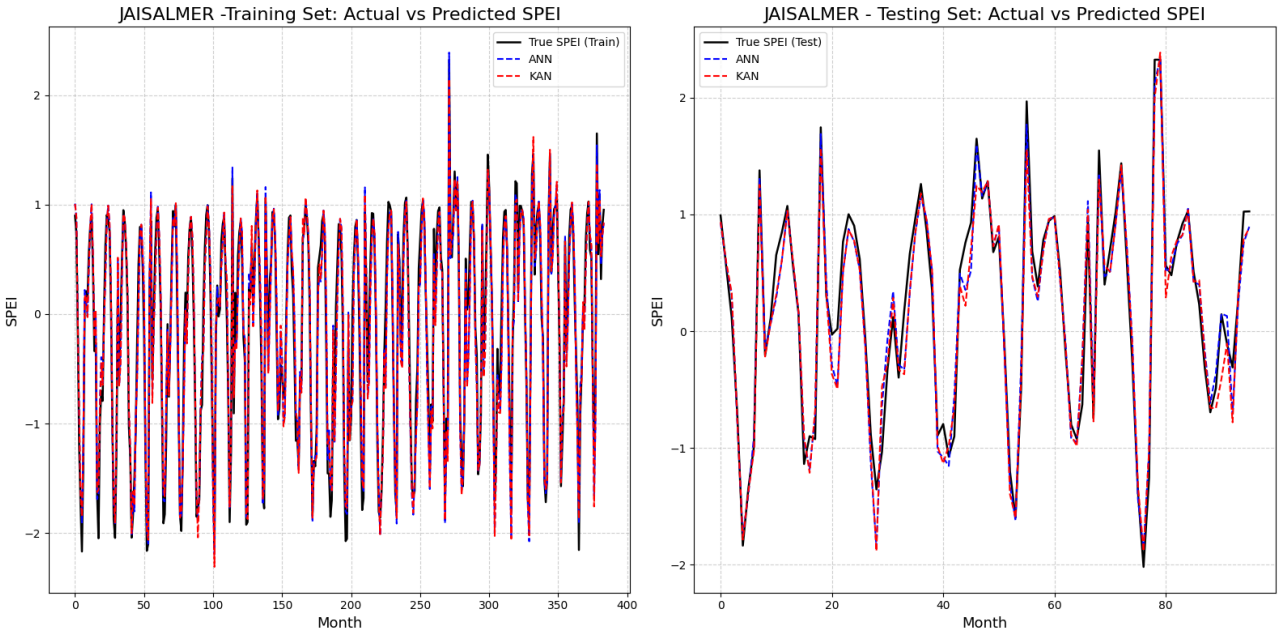

Figure 8. Observed versus predicted SPEI comparison for the Jaisalmer region

The KAN and ANN models effectively capture the fluctuations in drought intensity, demonstrating high accuracy and strong correspondence with observed values.

The time series plot for the different regions during the training and the testing period for the ANN and KAN model successfully captures the variations in the SPEI. It compares the observed SPEI with predicted SPEI from both the models with respect to time. During the training period both the models follow the true SPEI, capturing the temporal variations. During the testing period, the models predict SPEI with greater accuracy, indicating that the model works well with the unseen data. The predicted SPEIs are closer to the actual SPEIs. The presence of small deviations can be observed for the extreme values of the SPEI, but the overall pattern is well captured.

The scatter plot further confirms that; both the models have similar and high predictive capability reproducing the SPEI. Small deviations can be

observed when SPEI is around -2, indicating the need of more training samples. The values are clustering around the diagonal indicating that neither model exhibits major bias concluding that the ANN and KAN model performances are equivalent.

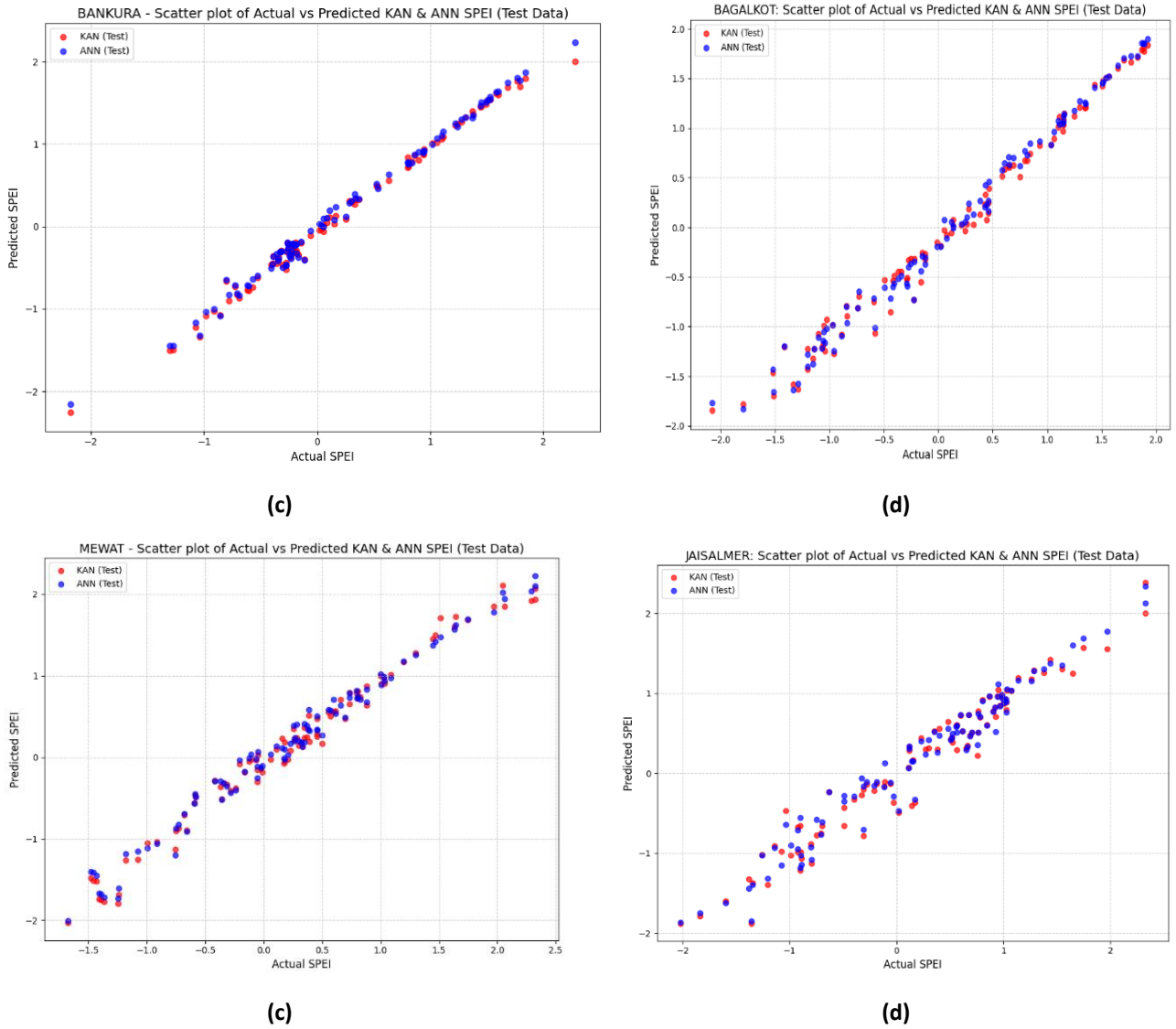

Figure 9. Scatter plots of observed versus predicted SPEI values for four study regions using KAN and ANN models during testing:(a) Bankura, (b) Bagalkot, (c) Mewat, and (d) Jaisalmer

The red and blue markers represent predictions from the KAN and ANN models, respectively. All plots show strong alignment to the diagonal, indicating that both models effectively capture drought variability with high predictive accuracy.

4. Conclusion

This study establishes the Kolmogorov Arnold Network as another learning framework for drought prediction. There are very few applications of KAN models for the drought prediction. The application 'tanh' as the activation function is introduced in this study to reduce the computation difficulties instead of using spline functions and still preserving the KAN additive structure This research compares the performance of the ANN and the KAN models for drought prediction for the districts Bankura, Mewat, Bagalkot and Jaisalmer of India which are highly vulnerable to droughts using Standardised Precipitation Evapotranspiration Index. Both the models successfully captures the non-linear relationship between the input variables and the target variable, SPEI. The evaluation metrics including RMSE (less than 0.21) and R^2 (more than 0.94) indicates both ANN and KAN model achieves high degree of accuracy. Despite KAN being a recently developed model, it shows a high accuracy and is a robust alternative to traditional ANN model. Although the KAN and ANN model shows

promising results, the study uses only three inputs, we can include other input variables, such as soil moisture, land surface temperature into the framework. Other deep learning models can be developed to predict droughts.

References

[1] Trends in drought occurrence and severity at mid-latitude European stations (1951–2015) estimated using standardized precipitation (SPI) and precipitation and evapotranspiration (SPEI) indices Paulina Dukat1 Ewa Bednorz2 Klaudia Ziemblińska1 Marek Urbaniak1 Received: 9 March 2020 / Accepted: 2 January 2022 / Published online: 22 January 2022

[2] Hansen, J., Sato, M., Ruedy, R., Lo, K., Lea, D. W., & Medina-Elizade, M. (2006). Global temperature change. *Proceedings of the National Academy of Sciences of the United States of America*, *103*(39), 14288–14293. https://doi.org/10.1073/pnas.0606291103

[3] Hosseinizadeh, A., SeyedKaboli, H., Zareie, H. *et al.* Impact of climate change on the severity, duration, and frequency of drought in a semi-arid agricultural basin. *GEOENVIRON DISASTERS* **2**, 23 (2015). https://doi.org/10.1186/s40677-015-0031-8

[4] Kuśmierek-Tomaszewska, R., & Żarski, J. (2021). Assessment of Meteorological and Agricultural Drought Occurrence in Central Poland in 1961–2020 as an Element of the Climatic Risk to Crop Production. *Agriculture*, *11*(9), 855. https://doi.org/10.3390/agriculture11090855

[5] Chiang F, Mazdiyasni O, AghaKouchak A. Evidence of anthropogenic impacts on global drought frequency, duration, and intensity. Nat Commun. 2021 May 12;12(1):2754. doi: 10.1038/s41467-021-22314-w. PMID: 33980822; PMCID: PMC8115225.

[6] D. A. Wilhite and M. H. Glantz, Understanding the drought phenomenon: The role of definitions, Water Int., 1985, 10(3), 111–120.

[7] A. K. Mishra and V. P. Singh, A review of drought concepts, J. Hydrology., 2010, 391(1–2), 202–216, https://doi.org/10.1016/j.jhydrol.2010.07.012.

[8] Nandgude, N., Singh, T. P., Nandgude, S., & Tiwari, M. (2023). Drought Prediction: A Comprehensive Review of Different Drought Prediction Models and Adopted Technologies. *Sustainability*, *15*(15), 11684. https://doi.org/10.3390/su151511684

[9] Trenberth, K. E., Dai, A., Van Der Schrier, G., Jones, P. D., Barichivich, J., Briffa, K. R., & Sheffield, J. (2014). Global warming and changes in drought. Nature Climate Change, 4(1), 17–22.

[10] Harris, I., Osborn, T. J., Jones, P., & Lister, D. (2020). Version 4 of the CRU TS monthly high-resolution gridded multivariate climate dataset. Scientific Data, 7(1), 109.

[11] Funk, C. C., Peterson, P. J., Landsfeld, M. F., Pedreros, D. H., Verdin, J. P., Rowland, J. D., & Michaelsen, J. (2015). The climate hazards infrared precipitation with stations—a new environmental record for monitoring extremes. Scientific Data, 2, 150066.

[12] **McKee, T. B., Doesken, N. J., & Kleist, J. (1993).** The relationship of drought frequency and duration to time scales. *Proceedings of the 8th Conference on Applied Climatology*, 17–22 January 1993, Anaheim, California. American Meteorological Society, Boston, MA, pp. 179–184.

[13] **Vicente-Serrano, S. M., Beguería, S., & López-Moreno, J. I. (2010).**A multiscalar drought index sensitive to global warming: The Standardized Precipitation Evapotranspiration Index. *Journal of Climate*, **23**(7), 1696–1718. https://doi.org/10.1175/2009JCLI2909.1

[14] **Alley, W. M. (1984).**The Palmer Drought Severity Index: Limitations and assumptions. *Journal of Climate and Applied Meteorology*, **23**(7), 1100–1109. https://doi.org/10.1175/1520-0450(1984)023<1100:TPDSIL>2.0.CO;2

[15] **Ostad-Ali-Askari, K., Shayannejad, M., Ghorbanizadeh-Kharazi, H., & Eslamian, S. (2018).** A review of drought indices. *International Journal of Constructive Research in Civil Engineering (IJCRCE)*, **4**(1), 1–14. https://doi.org/10.20431/2454-8693.0401001

[16] Praveen, B., & Sharma, P. (2019). Climate Change and its impacts on Indian agriculture: An Econometric analysis. *Journal of Public Affairs*, *20*(1). https://doi.org/10.1002/pa.1972

[17] Zarch, M. A. A., Sivakumar, B., & Sharma, A. (2015). Droughts in a warming climate: A global assessment of Standardized Precipitation Index (SPI) and the Standardized Precipitation

Evapotranspiration Index (SPEI). Journal of Hydrology, 526, 183–195.

[18] Li, X., He, B., Bai, X., Liao, Z., & Quan, X. (2015). Use of the Standardized Precipitation Evapotranspiration Index (SPEI) to Characterize the Drying Trend in Southwest China from 1982–2012. *Remote Sensing*, *7*(8), 10917–10937. https://doi.org/10.3390/rs70810917

[19] Belayneh, A., Adamowski, J., Khalil, B., & Ozga-Zielinski, B. (2014). Long-term SPI drought forecasting in the Awash River Basin in Ethiopia using wavelet neural networks and genetic algorithms. Applied Soft Computing, 25, 25–38.

[20] Khosravi, K., et al. (2018). A comparative assessment of different artificial intelligence models for drought prediction. Environmental Modelling & Software, 104, 1–20.

[21] Adnan, R. M., et al. (2021). Drought prediction using machine learning algorithms: ANN, SVM, and LSTM. Water Resources Management, 35(12), 3963–3983.

[22] Zhang, A., Jia, G., & Xia, J. (2020). Drought prediction using machine learning methods: A review. Earth-Science Reviews, 210, 103384. Ali, S., Li, D., Congbin, F., & Khan, F. (2022).

[23] Machine learning approaches for drought forecasting: A review. Environmental Modelling & Software, 156, 105487.

[24] Ramesh, Kokila & Iyengar, R.N. (2017). Forecasting Indian monsoon rainfall including within year seasonal variability. International Journal of Civil Engineering and Technology. 8. 390-399

[25] Kumudha, H. R. and Ramesh, K., A Gaussian and Gamma mixture model approach to Rainfall analysis in drought-prone regions of Karnataka. Mausam, Vol. 76 No. 4 (2025): Special Issue on "National Symposium on 75 years of Accomplishments of Mausam" https://doi.org/10.54302/mausam.v76i4.7014

[26] Kumudha, H. R. and Ramesh, K., Gaussian and Gamma Mixture Model Approach to Rainfall Analysis in Flood-Prone Regions of Karnataka. Communications on Applied Nonlinear Analysis, Vol. 32, No. 9s (2025)

[27] Ramesh, K., & Iyengar, R. N. (2017). *A non-Gaussian model for Indian monsoon rainfall*. International Journal of Research in Granthaalayah, **5**(4), 88–95. https://doi.org/10.5281/zenodo.556423

[28] Kumudha, H. R. and Ramesh, K., Statistical Analysis and Distribution Modeling of Rainfall Data in Flood-Prone Regions of Karnataka State. Tuijin Jishu/Journal of Propulsion Technology, Vol. 44, No. 4 (2023).

[29] Kumudha, H. R. and Ramesh, K., 2023, "Forecasting of Karnataka seasonal rainfall data using ANN approach", Journal of Survey in Fisheries Sciences, 10, 3, 3431–3448. https://doi.org/10.5281/zenodo.7709459.

[30] Kumudha, H. R. and Ramesh, K., et al. (2025) "Forecasting and Prediction of Seasonal Rainfall in Drought and Flood Affected Zones of Karnataka Using Artificial Neural Network (ANN)", Journal of Harbin Engineering University. ISSN: 1006-7043, Vol. 46 No. 12(Dec 2025): Issue 12 page No: 134 – 151.

[31] Ramesh K., and Kumudha H. R., 2019, "A review on forecasting Indian monsoon rainfall", International Journal of Innovative Science and Research Technology, Special Issue, AAM 2019, 9–14

[32] Ramesh K., and Iyengar R. N., 2017, "Rainfall distribution and probabilistic forecasting: A review", Journal of Earth System Science, 126, 3, 34. https://doi.org/10.1007/s12040-017-0810-6.

[33] Liu, Z. et al. (2024). *Kolmogorov–Arnold Networks*. arXiv:2404.19756. Vaca-Rubio, C.J.; Blanco, L.; Pereira, R.; Caus, M. Kolmogorov-Arnold Networks (KANs) for Time Series Analysis. *arxiv* **2024**, arXiv:2405.08790

[34] Wang, X., Liu, Z., & Zheng, J. (2024). Kolmogorov–Arnold Networks for function representation and learning. arXiv preprint arXiv:2406.02585.

[35] Zheng, J., Liu, Z., & Xu, M. (2024). Kolmogorov–Arnold Networks: A new paradigm for learning compositional functions. Advances in Neural Information Processing Systems (NeurIPS).

[36] Rajasthan Foundation, Jaisalmer, https://foundation.rajasthan.gov.in/rf/pdf/Jaisalmer.pdf (accessed 03.06.2025).

[37] Development Commissioner (MSME), Brief industrial profile of Mewat district, Ministry of Micro, Small and Medium Enterprises, Government of India, https://dcmsme.gov.in/dips/mewat.pdf (accessed 03.06.2025).

[38] Development Research Communication and Services Centre, Enhancing adaptive capacity and increasing resilience of small and marginal

farmers of Purulia and Bankura District, West Bengal to climate change, https://www.drcsc.org/ CCA/3/Docs/Study_Report.pdf (accessed 03.06. 2025).

[39] District Administration, Bagalkot District Official Website, https://bagalkot.nic.in/en/ (accessed 03.06.2025).

[40] National Aeronautics and Space Administration (NASA), POWER Data Access Viewer, NASA Langley Research Center, https://power.larc.nasa .gov/data-access-viewer/ (accessed 03.06.2025).

[41] K. Beven, A sensitivity analysis of the Penman–Monteith actual evapotranspiration estimates, J. Hydrology, 1979, 44(3–4), 169–190, https:// doi.org/10.1016/0022-1694(79)90130-6.

[42] A. S. Tefera, J. O. Ayoade and N. J. Bello, Comparative analyses of the SPI and SPEI as drought assessment tools in the Tigray Region, Northern Ethiopia, SN Appl. Sci., 2019, 1, 1265, https://doi.org/10.1007/s42452-019-1326-2.

[43] Hao, Z., & Singh, V.P. (2015). *Drought characterization from a multivariate perspective: A review*. Journal of Hydrology, 527, 668–678

[44] Pedregosa, F. et al. (2011). *Scikit-learn: Machine Learning in Python*. Journal of Machine Learning Research, 12, 2825–2830.

[45] Hyndman, R.J., & Athanasopoulos, G. (2021). *Forecasting: Principles and Practice* (3rd ed.). OTexts.

[46] McCulloch, W.S., & Pitts, W. (1943). *A logical calculus of the ideas immanent in nervous activity.* Bulletin of Mathematical Biophysics, 5(4), 115–133

[47] Schmidhuber, J. (2015). *Deep learning in neural networks: An overview.* Neural Networks, 61, 85–117

[48] Hornik, K., Stinchcombe, M., & White, H. (1989). *Multilayer feedforward networks are universal approximators.* Neural Networks, 2(5), 359–366.

[49] Rumelhart, D.E., Hinton, G.E., & Williams, R.J. (1986). *Learning representations by back-propagating errors.* Nature, 323, 533–536.

[50] Zhang, C., Bengio, S., Hardt, M., Recht, B., & Vinyals, O. (2021). *Understanding deep learning requires rethinking generalization.* Communications of the ACM, 64(3), 107–115.

[51] Kolmogorov, A. N. (1957). *On the representation of continuous functions of several variables by superposition of continuous functions of one variable and addition.* Doklady Akademii Nauk SSSR, 114(5), 953–956.

[52] Arnold, V. I. (1963). *On functions of three variables.* Doklady Akademii Nauk SSSR, 114, 679–681.

[53] Hecht-Nielsen, R. (1987). *Kolmogorov's mapping neural network existence theorem.* Proceedings of IEEE First International Conference on Neural Networks, 3, 11–14.

[54] Huber, P. J. (1964). *Robust estimation of a location parameter.* The Annals of Mathematical Statistics, 35(1), 73–101.

[55] Willmott, C. J., & Matsuura, K. (2005). *Advantages of the mean absolute error (MAE) over the root mean square error (RMSE) in assessing average model performance.* Climate Research, 30(1), 79–82

[56] Bozorgasl, Z., & Chen, H. (2024). *Wav-KAN: Wavelet Kolmogorov–Arnold Networks*. *arXiv preprint arXiv:2405.12832*. https://arxiv.org/abs/ 2405.12832